CellPress

Molecular Cell
Article

The Yeast ER-Intramembrane Protease Ypf1 Refines Nutrient Sensing by Regulating Transporter Abundance

Dönem Avci,[1,8] Shai Fuchs,[2,8] Bianca Schrul,[1,7] Akio Fukumori,[3,4] Michal Breker,[2] Idan Frumkin,[2] Chia-yi Chen,[1] Martin L. Biniossek,[6] Elisabeth Kremmer,[5] Oliver Schilling,[6] Harald Steiner,[3,4] Maya Schuldiner,[2,*] and Marius K. Lemberg[1,*]

[1]Zentrum für Molekulare Biologie der Universität Heidelberg (ZMBH), DKFZ-ZMBH Allianz, Im Neuenheimer Feld 282, 69120 Heidelberg, Germany
[2]Department of Molecular Genetics, Weizmann Institute of Science, Rehovot 7610001, Israel
[3]Adolf-Butenandt-Institut, Ludwig-Maximilians-Universität, 86336 Munich, Germany
[4]Deutsches Zentrum für Neurodegenerative Erkrankungen (DZNE), 86336 Munich, Germany
[5]Institute of Molecular Immunology, Helmholtz Center Munich, 81377 Munich, Germany
[6]Institut für Molekulare Medizin und Zellforschung and BIOSS Centre for Biological Signaling Studies, Albert-Ludwigs-Universität, 79104 Freiburg, Germany
[7]Present address: Department of Biology, Stanford University, Stanford, CA 94305, USA
[8]Co-first authors
*Correspondence: maya.schuldiner@weizmann.ac.il (M.S.), m.lemberg@zmbh.uni-heidelberg.de (M.K.L.)
http://dx.doi.org/10.1016/j.molcel.2014.10.012

SUMMARY

Proteolysis by aspartyl intramembrane proteases such as presenilin and signal peptide peptidase (SPP) underlies many cellular processes in health and disease. *Saccharomyces cerevisiae* encodes a homolog that we named yeast presenilin fold 1 (Ypf1), which we verify to be an SPP-type protease that localizes to the endoplasmic reticulum (ER). Our work shows that Ypf1 functionally interacts with the ER-associated degradation (ERAD) factors Dfm1 and Doa10 to regulate the abundance of nutrient transporters by degradation. We demonstrate how this noncanonical branch of the ERAD pathway, which we termed "ERAD regulatory" (ERAD-R), responds to ligand-mediated sensing as a trigger. More generally, we show that Ypf1-mediated posttranslational regulation of plasma membrane transporters is indispensible for early sensing and adaptation to nutrient depletion. The combination of systematic analysis alongside mechanistic details uncovers a broad role of intramembrane proteolysis in regulating secretome dynamics.

INTRODUCTION

Intramembrane proteolysis is an unusual process of peptide bond cleavage within cellular membranes, a hydrophobic environment that is only rarely exposed to water. In humans, 14 different intramembrane proteases have been identified that fall into four families: the site 2 metalloproteases, rhomboid serine proteases, the Rce1-type glutamyl proteases, and the GxGD aspartyl proteases (Lemberg, 2011; Manolaridis et al., 2013). The GxGD family of aspartyl proteases has been intensively studied, as its founding member, presenilin, forms the active subunit of the γ-secretase complex (De Strooper et al., 1998; Steiner et al., 2000; Wolfe et al., 1999), mutations in which underlie familial Alzheimer's disease (Levy-Lahad et al., 1995; Sherrington et al., 1995). A recent crystal structure of the archaeal GxGD protease MCMJR1 (Torres-Arancivia et al., 2010) revealed the architecture of the conserved presenilin fold (Li et al., 2013). A related group of enzymes, with the signal peptide peptidase (SPP) as the first identified example, also carries a presenilin fold but has an inverted topology of the membrane-embedded active site (Weihofen et al., 2002). SPP was originally characterized as being responsible for cleaving signal peptides to enable their clearance from the endoplasmic reticulum (ER) following their removal from nascent secretory proteins by signal peptidase (Weihofen et al., 2002). However, recently there has been growing evidence indicating that SPP has an equally important role in ER-associated degradation (ERAD) (Lee et al., 2010; Loureiro et al., 2006; Stagg et al., 2009), targeting damaged and unassembled proteins from the ER to the cytosolic proteasome (Bagola et al., 2011; Hampton and Sommer, 2012). Consistent with this, a novel therapeutic strategy to treat malaria targets the ERAD pathway of *Plasmodium falciparum* via inhibition of SPP, which is shown to be indispensible for ERAD in this disease vector (Harbut et al., 2012). However, the molecular function of SPP in ERAD is yet to be characterized, and cleaved substrates have not been identified. In humans, SPP was shown to interact with ERAD factors such as the E3 ubiquitin ligase TRC8 (Stagg et al., 2009). Interestingly, human SPP forms several distinct complexes (Schrul et al., 2010), and while the signal peptide-processing activity resides in a tetrameric 200 kDa complex (Miyashita et al., 2011; Schrul et al., 2010), we recently showed that it is the 500 kDa complex that also involves the ERAD machinery Derlin1 and TRC8 (Chen et al.,

2014). Since initially proteolytic substrates other than signal sequences could not be identified, it was suggested that SPP acts as a nonproteolytic scaffold for ERAD factors (Loureiro et al., 2006). However, we showed that SPP actively targets a type II membrane protein for proteasomal degradation (Chen et al., 2014), arguing that SPP has a central, direct, and active role in ERAD. Recently we have also identified a ubiquitin-dependent ERAD rhomboid protease in human cells that triggers degradation of unstable type I and polytopic membrane proteins (Fleig et al., 2012). The growing number of observations indicating involvement of intramembrane proteases in the ERAD pathway, alongside the fact that clipping has been shown for a variety of transmembrane (TM) proteins (Fleig et al., 2012; Huppa and Ploegh, 1997; Tyler et al., 2012), suggests that the role intramembrane proteolysis plays in membrane proteome maintenance is broader than has been so far appreciated.

To more generally address the role of GxGD proteases in the control of membrane protein homeostasis, we utilized the model eukaryote *Saccharomyces cerevisiae* to shed light on this protein family. In yeast, only four intramembrane proteases are predicted. By sequence homology only one, the uncharacterized open reading frame *YKL100C*, was predicted to be a GxGD protease (Weihofen et al., 2002). Here we show that *S. cerevisiae YKL100C*, which we named yeast presenilin fold 1 (*YPF1*), is indeed an ER-resident intramembrane protease that triggers degradation of polytopic membrane proteins. We demonstrate how Ypf1 synergizes with the E3 ubiquitin ligase Doa10 and the ERAD factor Dfm1 to control the abundance of the high-affinity zinc transporter Zrt1 in a zinc-dependent manner. Moreover, by genome-wide screening for substrates, we provide evidence that Ypf1 is a general posttranslational regulator of nutrient transporters. Using starvation assays we prove that Ypf1-mediated control of plasma membrane nutrient transporters is essential for efficient preparation for starvation and subsequent recovery. Our results uncover a so-far unrecognized tier of protein abundance control and open up new avenues of research on the role of GxGD intramembrane proteases in health and disease.

RESULTS

Ypf1 Is an ER-Resident Intramembrane Protease

In recent years, intramembrane proteases have been recognized as cellular switches that control a wide range of important pathways (Lemberg, 2011). Due to the high conservation of proteases in all living organisms, we decided to study the function of the uncharacterized GxGD protease homolog Ypf1 in *S. cerevisiae* (Weihofen et al., 2002). Whereas seven GxGD proteases are known in mammalian cells, Ypf1 is the only predicted aspartyl intramembrane protease in yeast (Figure 1A) (Ponting et al., 2002; Weihofen et al., 2002). Alignment of Ypf1 with human SPP, human Presenilin-1, and the archaeal GxGD protease MCMJR1 revealed significant sequence conservation for all nine TM segments (data not shown), suggesting that Ypf1 shares the presenilin fold with MCMJR1 and the metazoan GxGD proteases (Li et al., 2013). In addition to the characteristic YD and GLGD active site motifs located in the conserved TM domains 6 and 7, respectively, Ypf1 contains also the conserved QPALLYhhP motif characteristic of SPP-type aspartyl proteases (Figure 1B and see Figure S1 available online). Phylogenetic analysis using a stringent alignment of only the functionally important TM domains 6, 7, and 9 reveals that Ypf1 is the closest homolog to human SPP (Figures 1A and S1A) and a bona fide member of the GxGD protease family. Consistent with this similarity to human SPP, chromosomally tagged Ypf1-GFP was specifically localized to the perinuclear ER (as seen by the costaining pattern with the soluble ER marker dsRED-HDEL, which localizes to both the perinuclear and cortical ER) (Figure 1C). In addition, Ypf1 harbors two glycosylation sites in its N-terminal tail (Figure 1D), strongly suggesting that Ypf1 shares the SPP topology with its N terminus facing the ER lumen (Weihofen et al., 2002). Supporting its association with the GxGD branch of intramembrane proteases, detergent-solubilized Ypf1 was affinity captured by a biotinylated γ-secretase transition-state inhibitor, Merck C (Beher et al., 2003; Nyborg et al., 2004), in a highly specific manner (Figure 1E). Consistent results were observed for Ypf1-GFP, demonstrating that the C-terminal tag does not affect folding and the proteolytic activity (Figure S1B). Taken together, our results imply that Ypf1 is the yeast ER-resident intramembrane protease equivalent to vertebrate SPP.

Ypf1 Mediates Degradation of Zrt1

The close phylogenetic relationship of Ypf1 to the GxGD proteases drove us to utilize it as a model to uncover new substrates and functions of this protein family. Therefore, we compared the abundance of membrane proteins in ER-derived microsomes from control and *Δypf1* cells by quantitative proteomics. Since the strains used in this study are leucine auxotrophs, we chose metabolic labeling with deuterated leucine. The proteomic analysis identified 2,682 proteins, of which 2,095 were quantified based on differential isotope labeling. Although most proteins were equally abundant in both strains, for the high-affinity zinc transporter Zrt1 we detected three different peptides that showed a significant enrichment of 1.5- to 1.8-fold (p value = 0.002) in *Δypf1* cells compared to control cells (Figure 2A), suggesting that Ypf1 controls Zrt1 abundance in the ER. When we directly tracked Zrt1-RFP expression level by flow cytometry or western blotting, we found up to 4-fold increase in the intensity of Zrt1-RFP in *Δypf1* cells compared to control cells or Ypf1-GFP-tagged cells (Figures 2B and S2A). Consistent but slightly less pronounced effects were observed for fusions with two alternative fluorescent proteins (Figures S2B and S2C), demonstrating that the effect is caused by the specific properties of Zrt1 and not by tagging strategy. Likewise, cycloheximide-chase experiments of chromosomally HA-tagged Zrt1 revealed a 2-fold increase of the steady-state level at time point zero (Figure 2C). Moreover, the predominant form (a 50 kDa species) had twice as long a half-life in *Δypf1* cells compared to control cells (20 min relative to 10 min, respectively) (Figure 2C).

The molecular mass of Zrt1 slightly increases with time (Figures 2C and S2D–S2F), indicating modified glycosylation in the Golgi, as has been observed previously (Gitan et al., 1998). To focus our measurements on the ER pool of Zrt1 rather than later forms, we created a pulse of newly translated Zrt1 by expressing it from a galactose-inducible promoter and saw an

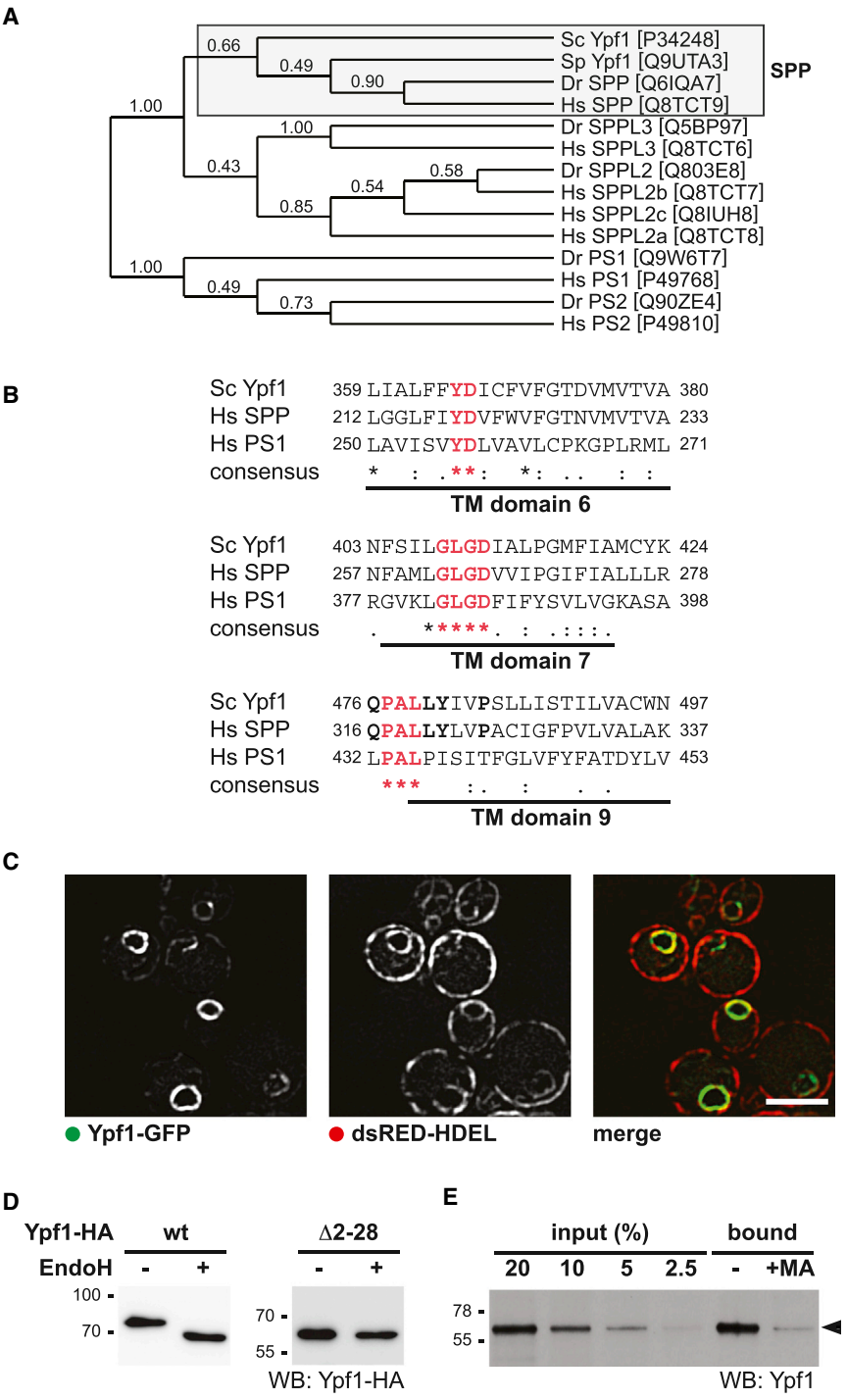

Figure 1. Ypf1 Is an ER-Resident GxGD Intramembrane Protease

(A) Phylogenetic tree of GxGD intramembrane proteases from *S. cerevisiae* (Sc), *S. pombe* (Sp), zebrafish (*D. rerio*, Dr), and human (*H. sapiens*, Hs). Dendogram is constructed by WAG bootstrap analysis of the multiple sequence alignment of TM domains 6, 7, and 9 shown in Figure S1. Swiss-Prot accession numbers are indicated in brackets; SPPL, SPP-like; PS, presenilin.

(B) Sequence alignments of Sc Ypf1, Hs SPP and Hs Presenilin-1 (PS1) showing conserved active site motives YD and GLDG located in TM domains 6 and 7, respectively, as well as the PAL motive.

(C) Fluorescent microscopy analysis of Ypf1 chromosomally tagged with GFP shows colocalization with dsRED-HDEL. Scale bar, 5 μM.

(D) Ypf1-HA is glycosylated as demonstrated by western blot analysis of Endoglycosidase H (EndoH)-treated cell extracts, whereas N-terminally truncated Ypf1-HA (Δ2-28) lacking both glycosylation sites N22 and N28 is not.

(E) CHAPSO-solubilized Ypf1 is affinity captured by a biotinylated γ-secretase inhibitor Merck C using streptavidin Sepharose beads. Addition of excess amounts of parental nonbiotinylated inhibitor compound L-685,458 (Merck A, MA) competes with binding.

See also Figure S1.

enhanced role of Ypf1 in degradation of this form both by cycloheximide chase (Figure S2D) and a promoter shutoff experiment (Figure S2E). To verify this effect, we used a *sec23-1* genetic background, at the restrictive temperature, to block COPII-mediated ER to Golgi transport (Baker et al., 1988) and retain Zrt1 in the ER. Indeed, when Zrt1 expression was induced under such conditions, it was detected only as the 50 kDa ER form (Figure 2D). Promoter shutoff and chase experiments under these conditions revealed that in Δ*ypf1* cells less than 20% of the ER pool of Zrt1 is degraded, whereas in control cells the level drops to 50% within 2 hr (Figure 2D), uncovering the dramatic extent of Ypf1-mediated degradation. Likewise, we observed Ypf1-dependent degradation of Zrt1 fused to an HDEL ER-retention signal (Figure S2F), demonstrating that the effect is not caused by unspecific accumulation of bulk protein cargo. We also found that the low-affinity zinc transporter Zrt2, which shares 67% sequence similarity, the same membrane topology, and similar abundance with Zrt1 (Gaither and Eide, 2001), was not stabilized in Δ*ypf1* cells (Figure 2D). This result highlights that any potential posttranslational regulatory role of Ypf1 on Zrt1 stability is specific and not a consequence of general protein accumulation in the ER. Moreover, promoter shutoff and chase experiments in a *sec23-1* strain deficient for the vacuolar proteases Pep4 and Prb1 showed similar degradation kinetics to the control strain (compare Figures 2D and S2G), whereas deletion of *ypf1* in the *sec23-1*Δ*pep4*Δ*prb1* background led to Zrt1 accumulation (Figure S2G). Taken together, these results show that Zrt1 turnover at ER is dependent only on Ypf1 and does not rely

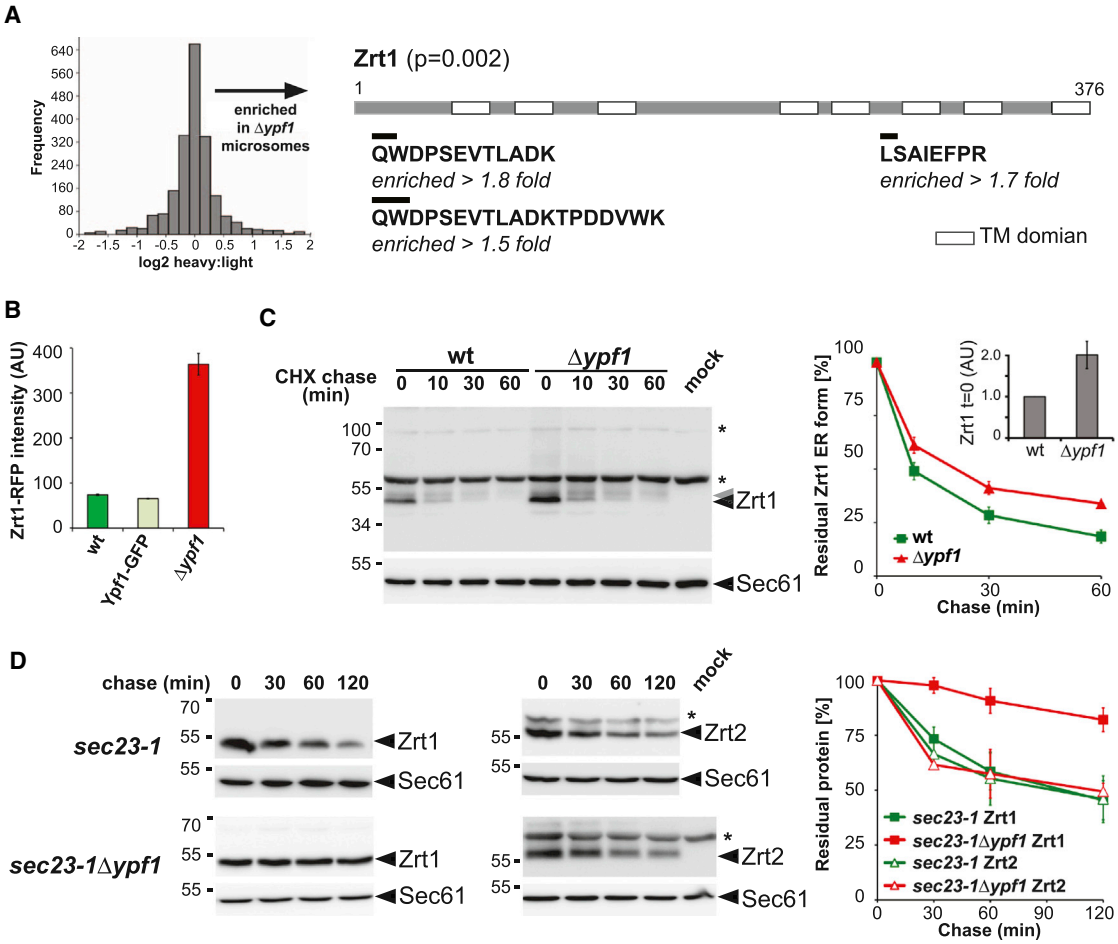

Figure 2. Ypf1 Degrades Zrt1

(A) Quantitative proteomic analysis of microsomes obtained from WT and *Δypf1* cells shows that most proteins are unaffected as demonstrated by the histogram of the distribution of fold-change values (left panel). For the polytopic membrane protein Zrt1, location and fold change of all identified peptides are shown (right panel).

(B) Flow cytometry for WT and *Δypf1* cells expressing chromosomally tagged Zrt1-RFP, showing elevated fluorescence intensity in *ypf1* deletion. Ypf1-GFP phenocopies Zrt1-RFP abundance of the WT strain.

(C) Cycloheximide (CHX) chase experiments with WT and *Δypf1* cells expressing Zrt1 chromosomally tagged at its C terminus show slower degradation kinetics upon *ypf1* deletion. Western blot quantification for the 50 kDa ER form of Zrt1 is shown on the right (means ± SEM, n = 3). Sec61 is used as loading control. Asterisk, crossreacting protein; gray triangle, Zrt1 with complex-type glycans.

(D) Promoter shutoff chase experiments in *sec23-1* background show a significant delay in degradation of Zrt1 harboring an N-terminal HA-tag, whereas the related Zrt2 construct was not stabilized upon *ypf1* deletion (means ± SEM, n = 3). Asterisk, crossreacting protein.

See also Figure S2.

on the regulated endocytosis and vacuolar degradation pathways involved in inactivation of the plasma membrane pool (Gitan et al., 1998).

Since we detected an increase of endogenous untagged Zrt1 levels by mass spectrometry (Figure 2A) and HA-tagged Zrt1 is fully functional as shown by rescue of the growth defect of Δ*zrt1* cells under zinc-limiting conditions (Figure S2H), our results demonstrate that Ypf1-mediated degradation is not merely an artifact of tagging. More interestingly, it suggests that Ypf1 regulates the abundance of folding-competent, ER-localized Zrt1 rather than a misfolded species, and that Zrt1 degradation serves a regulatory role rather than to eliminate aberrant or unassembled species.

Ypf1 Binds Zrt1 and Requires Proteolytic Activity to Cause Its Degradation

It has been shown that ERAD machinery degrades native substrates such as the HMG-CoA reductase Hmg2, which is controlled by a sterol-dependent feedback regulation (Gardner and Hampton, 1999). In an opposite manner, binding of toxic heavy metals to a degradation signal in the cadmium transporter Pca1 enables it to escape from ERAD to the plasma membrane, where it detoxifies the cell (Adle et al., 2009). We therefore postulated that Ypf1 is an ERAD factor that posttranslationally regulates the stability of Zrt1. If indeed Ypf1 is an ERAD factor, then its ability to perform intramembrane proteolysis should serve as a means to facilitate Zrt1 degradation. Although

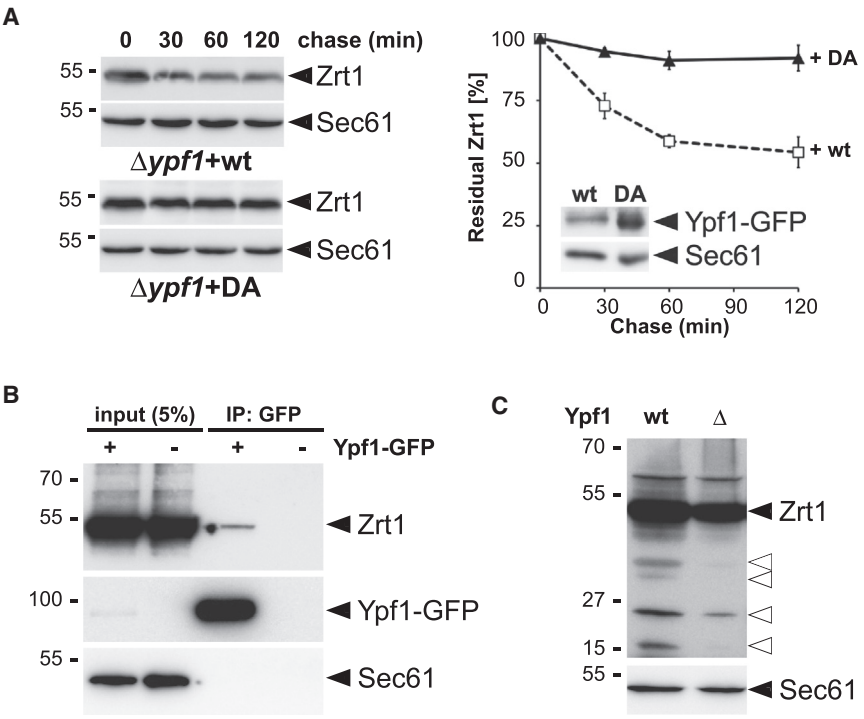

Figure 3. Ypf1 Is an Active ERAD Protease

(A) Degradation of Zrt1 in the ER of *sec23-1Δypf1* cells can be rescued by GFP-tagged Ypf1, but not by its catalytic mutant (DA) (means ± SEM, n = 3).

(B) Immunoprecipitation (IP) with anti-GFP antibody from digitonin-solubilized microsomes of cells expressing Ypf1-GFP and Zrt1 and western blot (WB) analysis with indicated antibodies.

(C) In presence of the proteasome inhibitors lactacystin (20 μM) and clasto-lactacystin β-lactone (20 μM) in *sec23-1Δpdr5* cells (WT) expressing Zrt1-HA, N-terminal fragments with the apparent molecular weight of 38, 35, and 15 kDa are detected (open triangles), whereas in *sec23-1Δpdr5Δypf1* cells (Δ) a different pattern is observed.

intramembrane proteases commonly cleave single-spanning membrane proteins, we recently observed that the ERAD rhomboid protease RHBDL4 cleaves polytopic membrane proteins at several positions, thereby triggering their degradation (Fleig et al., 2012). To test whether Ypf1 protease activity is similarly directly involved in degradation of the multispanning membrane protein Zrt1, we performed rescue experiments on the Δ*ypf1* strain with plasmid-born expression of GFP-tagged Ypf1^{WT} or a catalytically inactive Ypf1^{D411A} mutant (see Figure 1B for annotation of the active site). Promoter shutoff and chase experiments in the presence of the *sec23-1* transport block showed that the WT protease rescued Zrt1 degradation in Δ*ypf1* cells, whereas the catalytic mutant could not (Figure 3A). Consistent with a role of Ypf1 as an ERAD protease, we observed coimmunoprecipitation of Zrt1 with Ypf1-GFP (Figure 3B), whereas the unrelated polytopic ER protein Sec61 did not copurify (Figure 3B). Moreover, inhibition of the proteasome stabilized several N-terminal Zrt1 cleavage fragments in control cells, whereas a different pattern of minor degradation intermediates was observed in Δ*ypf1* cells (Figure 3C). Taken together, our results strongly support the model of proteolysis-driven degradation of Zrt1 catalyzed by Ypf1.

Ypf1 Defines a Dfm1- and Doa10-Dependent ERAD Branch

If Ypf1 plays an active and direct role in the degradation of Zrt1, then we wondered how its activity is controlled. To uncover its cooperating factors, we tested which additional ERAD proteins affect Zrt1 turnover. First, we looked at the two yeast derlins that link ubiquitination with dislocation of ERAD substrates by an unknown mechanism (Bagola et al., 2011; Hampton and Sommer, 2012). We analyzed degradation kinetics in *sec23-1* strains deficient for either Der1 or Dfm1 (Figure 4A). Consistent with its known role in ERAD of soluble substrates (Carvalho et al., 2006), *der1* deletion had no effect on Zrt1 turnover. However, deletion of *dfm1* caused a subtle but reproducible delay in Zrt1 degradation (Figures 4A, S3A, and S3B). Deletion of *dfm1* and *der1* together did not show any enhancement of the loss-of-function phenotype (Figure 4A), indicating that Dfm1 plays a specific role in Zrt1 turnover. Similar stabilization in *Δdfm1* cells has been observed for the degradation of the polytopic model ERAD substrate Ste6* (Stolz et al., 2010). Consistent with the idea of Ypf1 and Dfm1 having a shared role, we observed a robust physical interaction of Ypf1-GFP with chromosomally HA-tagged Dfm1, but not Der1 (Figures 4B and S3C).

We next tested which of the two ER-localized E3 ubiquitin ligases, Hrd1 or Doa10, functions with Ypf1. *Hrd1* deletion did not affect Zrt1 turnover, whereas *doa10* deletion blocked Zrt1 degradation (Figures 4C, S3A, and S3B). Taken together, our results indicate that Ypf1-mediated ERAD of Zrt1 depends on a noncanonical branch of the ERAD pathway. Consistent with this idea, we observed high-molecular-weight complexes of Ypf1 by blue native gel electrophoresis (Figures S3D and S3E).

Since we found Doa10 to be the E3 ubiquitin ligase driving Zrt1 degradation and since Doa10 is known to recognize cytosolic lesions of ERAD substrates (Carvalho et al., 2006), we hypothesized that a cytoplasmic region of Zrt1 serves as a degradation signal. It stood to reason that the region serving as the Doa10 degron for Zrt1 is the cytosolic loop 3, which is known to regulate monoubiquitination and endocytosis in a zinc-dependent manner when Zrt1 is found on the plasma membrane (Gitan et al., 2003). To assess the role of this putative metal-sensitive degron, we analyzed degradation kinetics of the Zrt1^{K195R} mutant lacking the invariant lysine for ubiquitin-triggered endocytosis (Gitan and Eide, 2000). Promoter shutoff and chase experiments of Zrt1^{K195R} expressed in *sec23-1* cells showed that this lysine is also essential for degradation of the ER-retained Zrt1 (Figure 4D). Taken together with the putative metal-binding properties of loop 3 (Gaither and Eide, 2001), this result suggests that Zrt1 has a zinc-sensitive degron that is recognized by the Doa10-, Dfm1-, and Ypf1-dependent arm of the ERAD pathway (Figure 4E).

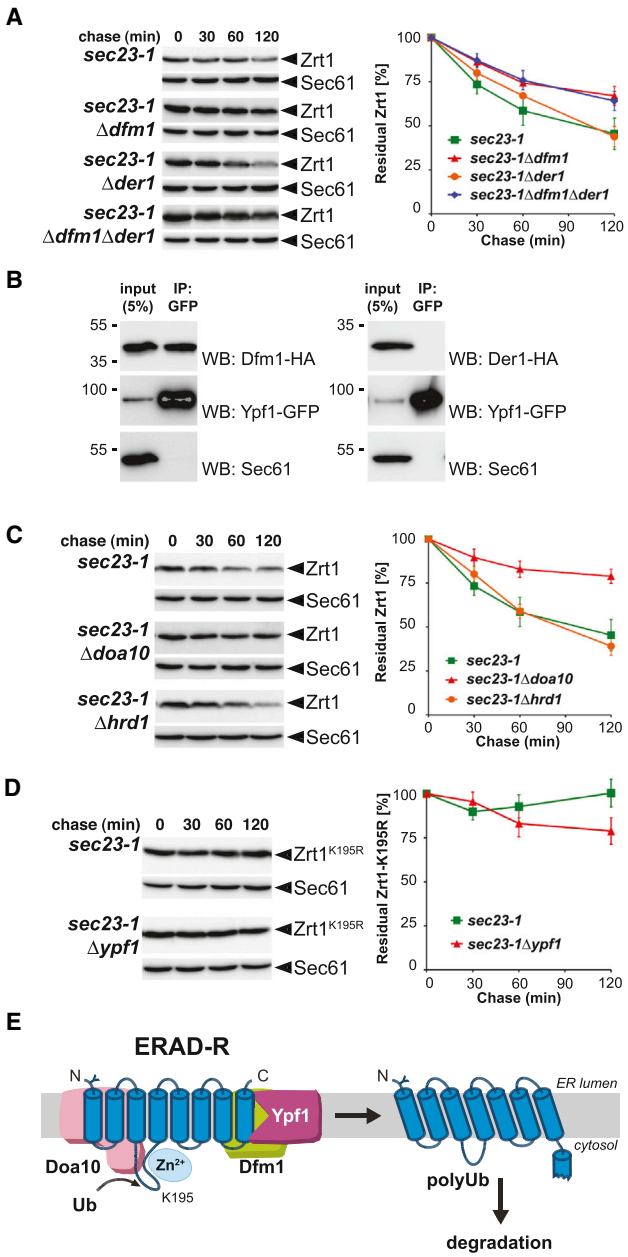

Figure 4. Ypf1-Mediated Degradation Utilizes Dfm1 and Doa10

(A) Promoter shutoff chase experiments in *sec23-1* background show a delay in the degradation of Zrt1 upon *dfm1* deletion but not *der1*. Western blot quantification for residual Zrt1 is shown on the right (means ± SEM, n = 3).

(B) Immunoprecipitation (IP) with anti-GFP antibody from digitonin-solubilized microsomes of cells expressing Ypf1-GFP and chromosomally tagged Dfm1-HA or Der1-HA and western blot (WB) analysis.

(C) Degradation of ER-resident Zrt1 is dependent on Doa10 but not Hrd1 (means ± SEM, n = 3).

(D) Promoter shutoff chase experiments in *sec23-1* background assessing degradation kinetics of $Zrt1^{K195R}$ (means ± SEM, n = 3).

(E) Model for ERAD-R-mediated regulation of Zrt1. At high zinc (Zn^{2+}) level, Doa10 links ubiquitin (Ub) to K195 in the cytosolic loop 3 of Zrt1, and Ypf1 drives degradation by a clipping event that destabilizes the Zrt1 protein fold, leading to efficient degradation.

See also Figure S3.

To date, four ERAD branches have been named; ERAD-L takes care of misfolded luminal substrates, ERAD-M degrades misfolded membrane lesions, and ERAD-C tags ER proteins that are misfolded on the cytosolic surface of the membrane for degradation (Carvalho et al., 2006; Hampton and Sommer, 2012). Recently we have named prERAD, a Doa10-dependent branch of ERAD that deals with preinserted endomembrane proteins (Ast et al., 2014). Consistent with a unique regulatory role of Ypf1-triggered degradation of Zrt1, turnover of classical ERAD substrates, namely CTL* (ERAD-L), Sec61-2L (ERAD-M), and CFTR (ERAD-C) (Carvalho et al., 2006; Kohlmann et al., 2008; Zhang et al., 2001), were not affected by *ypf1* deletion (Figures S3F–S3H). Likewise, the unstable loss of function mutant Zrt1Δ1 caused by a deletion in the potential zinc-binding loop 3 (Gitan et al., 2003) was degraded in a Ypf1-independent manner (Figure S3I). Taken together, our results reveal a Ypf1-, Dfm1-, and Doa10-dependent regulatory pathway that does not fall into any of the classical categories; hence we have named it ERAD-R for "ERAD regulatory" (Figure 4E).

Zinc-Sensitive Posttranslational Abundance Control of Zrt1

Since ERAD-R of Zrt1 was highly dependent on the putative zinc-binding loop, and since our data suggest that the function of ERAD-R is to regulate the abundance of Zrt1 rather than monitor its quality, we wondered whether the posttranslational abundance regulation at the ER is activated by cellular zinc availability. In order to test this, we studied the stability of Zrt1 under replete (2 mM), intermediate (20 μM), and zinc-free conditions. Consistent with previous report, the total pool of Zrt1 was rapidly degraded in the presence of zinc, whereas in zinc-free medium Zrt1 showed an increased half-life (Figure S4) (Gitan et al., 1998). While this is partially attributed to vacuolar degradation in response to zinc-triggered endocytosis of the Zrt1 plasma membrane pool (Gitan and Eide, 2000), we hypothesized that Ypf1-mediated degradation serves as an additional regulatory node. Promoter shutoff and chase experiments in the *sec23-1* strain showed that, indeed, in the absence of zinc, Zrt1 turnover at the ER comes to a halt, while in zinc-replete conditions Zrt1 degradation is accelerated (Figure 5A). Consistent with this, in the presence of high zinc, *ypf1* deletion caused a dramatic stabilization of Zrt1-RFP, whereas upon zinc starvation there was no significant difference in RFP intensity between the control and *Δypf1* strain (Figure 5B). These results indicate that Ypf1 degrades Zrt1 only at zinc-replete conditions. However, under limited zinc concentrations, when Zrt1 must be displayed on the plasma membrane, it is stabilized. The finding that degradation of Zrt1 via the ERAD-R pathway increases only under zinc repletion highlights how different it is from classical ERAD that degrades either folding-deficient mutants or orphan subunits of multiprotein complexes (Bagola et al., 2011).

Posttranslational Regulation by Ypf1 Is Required for Accurate Zinc Sensing and Rapid Adaptation to Varying Nutrient Availability

Why would yeast synthesize Zrt1 to immediately send it for degradation? For several nutrients, yeast express both low- and high-affinity transporters. Recently the enigma of why

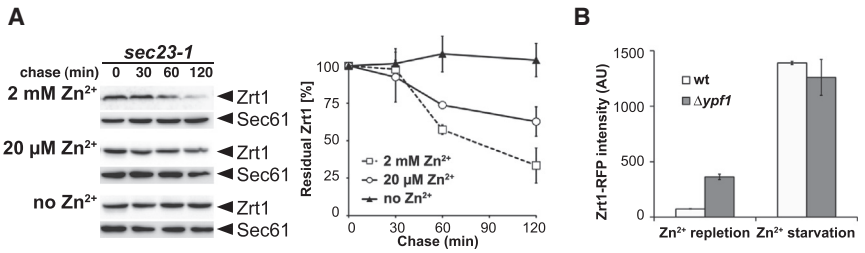

Figure 5. Ypf1-Mediated ERAD Is Sensitive to Zinc Concentration

(A) Zrt1 stability in *sec23-1* background under varying zinc concentrations. Western blot quantification for residual Zrt1 is shown on the right (means ± SEM, n = 3).

(B) Flow cytometry for WT and *Δypf1* cells expressing chromosomally tagged Zrt1-RFP under zinc repletion or zinc starvation. Bar graphs represent RFP intensity (means ± SEM, n = 3).

See also Figure S4.

such dual transporter systems are required has been solved (Levy et al., 2011). During growth in rich medium it is important to display only low-affinity transporters on the cell surface so that a decline in nutrient flux through the low-affinity transporters allows sensing of ensuing starvation. Once sensing has commenced, a starvation response is initiated to adapt. As a component of the starvation response, rapid upregulation of high-affinity transporters enables uptake of as much of the dwindling nutrient as possible. Hence, cells have evolved an intricate transcriptional control to repress high-affinity transporters under nutrient replete while upregulating them during nutrient deplete conditions (Radisky and Kaplan, 1999). Obviously, evolving additional posttranslational mechanisms that safeguard the transcriptional control as well as enable rapid changes in cell-surface expression is of immense benefit to the cell. We posited that Ypf1 activity as an ER intramembrane protease could provide these exact functions.

It has been shown that when cells constitutively express the high-affinity zinc transporter Zrt1 they fail to sense intermediate decline of zinc, resulting in worse performance when concentration further drops to severe starvation (Levy et al., 2011). If the role of Ypf1 is indeed to safelock Zrt1 from getting to the plasma membrane during nutrient-replete conditions, then we hypothesized that in its absence we will find a similar adaptation defect even under the normal transcriptional control. First, we ruled out Ypf1's role in transcriptional regulation of Zrt1 by observing identical levels of zinc-sensitive transcription factor Zap1-mCherry in control and *Δypf1* cells (Figure S5A). Then, we measured the ability of the *Δypf1* strain to sense depletion in zinc levels and induce preparation for zinc starvation based on *ZRT1* promoter activity (Levy et al., 2011). Reassuringly, *Δypf1* cells sensed full zinc repletion and depletion with a response comparable to control cells (Figure 6A). However, at an intermediate zinc concentration (5 μM), *Δypf1* cells induced a significantly lower transcriptional response to ensuing zinc starvation. This demonstrates that in the absence of Ypf1, increased Zrt1 activity masks the ability of the cells to sense nutrient limitation, thus reducing the cell's ability to prepare for starvation.

In order to test the role of Ypf1 in preparation for starvation, we diluted *Δypf1* and control cells from synchronized logarithmic growth into zinc starvation with or without preceding preparation at an intermediate zinc concentration (Figure 6B). Interestingly, when cells experienced an abrupt entry to starvation, there was no effect of losing Ypf1 activity, and both strains showed the same growth profile (Figure S5B). However, when the cells were allowed to prepare for starvation by exposing them to a gradual decrease in nutrients, unlike control cells, *Δypf1* cells grew as if they did not undergo a preparation phase at all (Figure 6C). These results indicate that in the absence of Ypf1, the increased level of Zrt1 on the plasma membrane hampers the yeast cell's ability to accurately sense a reduction in external zinc (preparation) and properly activate the zinc starvation response in a timely manner. The second anticipated consequence of a failure in preparation for starvation was shown to be a lag in exit from starvation (Levy et al., 2011). Strikingly, upon repletion by transfer into complete medium, *Δypf1* cells that were given an opportunity to prepare for starvation did not prepare correctly, as shown by lagged recovery (Figure 6D), whereas cells that were exposed to starvation without preparation showed indistinguishable growth from a control strain (Figure S5C). To validate this, we performed a competitive fitness assay between control cells and GFP-labeled *Δypf1* cells analyzing the changes in relative fitness of the population by flow cytometry (Levy et al., 2011). Indeed, when exiting starvation after preparation (Figure 6B), *Δypf1* cells had a fitness disadvantage compared to the control cells, leading to a decrease of their relative fraction in the population (fitness disadvantage of 2.6%, see Supplemental Experimental Procedures) (Figure 6E). As expected, a cell pool lacking starvation preparation showed indistinguishable growth, reassuring that Ypf1 is only essential for optimal growth in gradual fluctuation of nutrient concentrations. Consistent fitness defects were observed for *Δdfm1* and *Δdoa10* strains (Figures S5D and S5E). Taken together, these results show that the posttranslational regulation of Zrt1 abundance by ERAD-R is essential as a double safe mechanism to eliminate residual Zrt1 from the plasma membrane, allowing optimal sensing of intermediate zinc concentrations and accurate induction of the starvation response.

Posttranslational Regulation by Ypf1 Is a General Theme in Nutrient Sensing

Our results so far showed that ERAD-R targets Zrt1 in a nutrient-dependent manner. In order to address the scope of this mechanism for additional transporters, we utilized a high-content screening approach (Breker et al., 2013) to measure the levels of 5,330 yeast proteins from the GFP fusion library (Huh et al., 2003) in control and *Δypf1* cells. In addition to some proteins changing their localization (Table S1), the most impressive change in *Δypf1* cells was a significant upregulation of proteins assigned to gene ontology of transport function (Figure S6A). This indicates that Ypf1 has a central role in downregulating transport processes in general. Indeed, a cumulative distribution

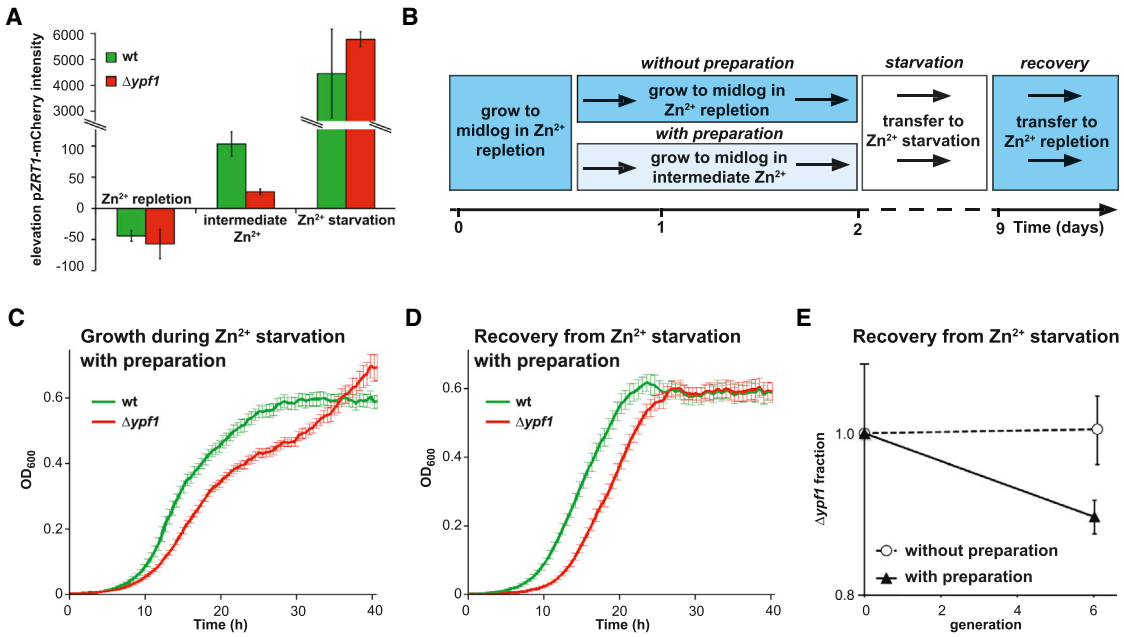

Figure 6. Deletion of *ypf1* Impairs Preparation for Zinc Starvation

(A) mCherry reporter assay for *ZRT1* promoter activity under varying zinc concentrations. Bar graphs represent the change in mCherry intensity from t = 0 hr to t = 23 hr (means ± SEM, n = 3).

(B) Experimental outline for starvation and recovery assays shown in (C), (D), and Figures S5B and S5C.

(C) Growth curves for WT and *Δypf1* cells during zinc starvation with preparation at intermediate zinc condition (means ± SD, n = 42).

(D) Growth curves for WT and *Δypf1* cells during recovery from zinc starvation with preparation at intermediate zinc condition (means ± SD, n = 42).

(E) Competition assay for WT and *Δypf1* cells during recovery from zinc starvation with or without preparation. Graph represents the relative fraction of *Δypf1* cells to WT cells grown in same culture, in log2 scale (means ± SEM, n = 3).

See also Figure S5.

function of all 27 high-affinity transporters in our screen showed them to be preferentially affected (Figure 7A), with 21 out of 27 high-affinity transporters showing increased intensity in the *Δypf1* background (Table S2). Manual analysis of selected candidates such as the amino acid transporters Dip5 and Mmp1, the ion transporters Ftr1 and Ctr1, and the glucose transporter Hxt2 by flow cytometry confirmed elevated abundance in *Δypf1* cells (Figure S6B). To see if our screen held predictive power, we measured the level of the high-affinity phosphor transporter missing in the GFP fusion library, Pho84-Venus, and revealed an increase of cellular level by 59% upon *ypf1* deletion (Figure 7B). Consistent with a general role of Ypf1 in posttranslational regulation of high-affinity transporters to enable sensing of starvation, growth competition upon recovery from phosphor starvation following preparation revealed that *Δypf1* has a 4.7% fitness defect compared to the control strain (Figure 7C). Likewise, *Δypf1* cells show a lag phase of 1.25 hr following amino acid depletion, both in full nitrogen starvation and in repletion (Figure S6C), indicating that the elevated levels observed for amino acid transporters such as Dip5 (Figure S6B) similarly lead to an adaptation defect. Taken together, our results show that *Δypf1* cells have a general problem in sensing upcoming nutrient restriction and that this affects their ability to respond to starvation cues. This places Ypf1 as a hub in the regulated posttranslational abundance control of plasma membrane transporters.

DISCUSSION

Here we showed that *S. cerevisiae* Ypf1 is an ER-resident aspartyl intramembrane protease with a presenilin fold, and investigated its role in regulating abundance of plasma membrane transporters. Using a candidate approach we identified the E3 ligase Doa10 and the putative substrate receptor Dfm1 as Ypf1 cofactors, defining a branch of the ERAD pathway, which we termed ERAD-R (ERAD regulatory) (Figures 4E and 7D). Taken together with a microscopy-based systematic proteome analysis and starvation assays, our findings suggest an essential role for Ypf1 in posttranslational abundance control of nutrient transporters. We propose, therefore, that Ypf1 is a central component of the starvation-sensing network in yeast.

Although SPP was originally discovered by its role in clearing signal peptides from the ER membrane (Weihofen et al., 2002), it is currently unclear whether this is in fact the primary role or whether its main function is the control of membrane protein homeostasis. Our analysis of yeast Ypf1 reveals a prominent role in degradation of polytopic membrane proteins. We note, however, that our substrate search was limited to full-length proteins and did not include signal peptides. Although a previous biochemical study showed that the detergent-solubilized *Schizosaccharomyces pombe* Ypf1 homolog can cleave signal peptides (Narayanan et al., 2007), an important question remaining is whether Ypf1 also degrades signal peptides in vivo.

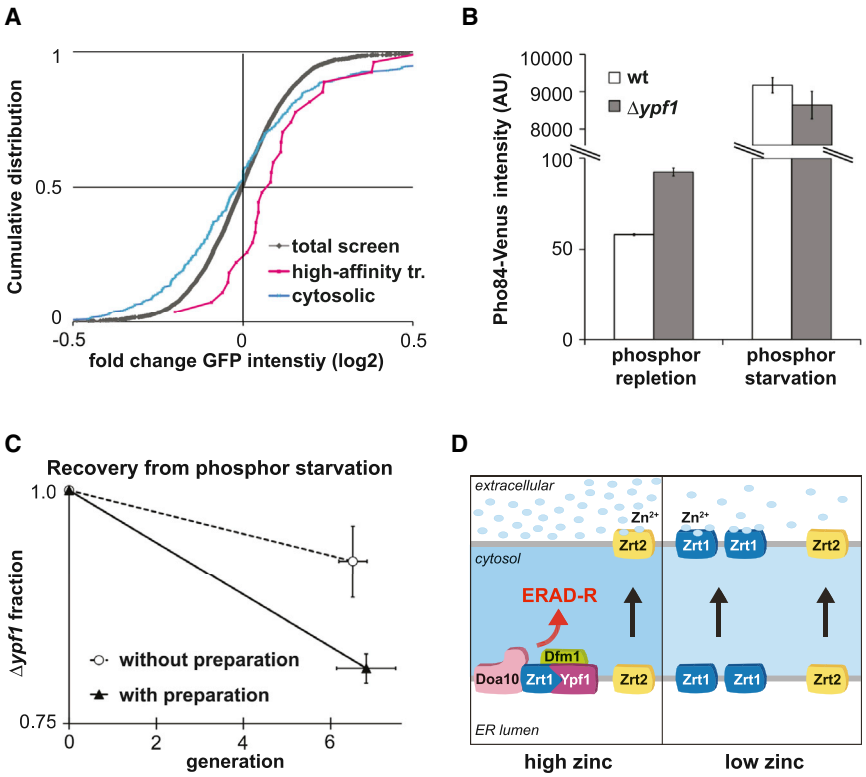

Figure 7. Ypf1 Is a General Regulator for Abundance of High-Affinity Transporters

(A) Cumulative distribution analysis of intensity changes in the GFP library screen in *ypf1* deletion strains shows specific elevation in levels of high-affinity transporters compared to the entire library. Cytosolic proteins not expected to interact with Ypf1 are shown as control.

(B) Flow cytometry for WT and *Δypf1* cells expressing chromosomally tagged Pho84-Venus under phosphor repletion or phosphor starvation. Bar graphs represent Venus intensity (means ± SEM, n = 3).

(C) Competition assay for WT and *Δypf1* cells during recovery from phosphor starvation with or without preparation. Graph represents the relative fraction of *Δypf1* cells to WT cells grown in same culture, in log2 scale (means ± SEM, n = 3).

(D) Model for ERAD-R-mediated regulation of high-affinity nutrient transporters. During growth at zinc-replete conditions, Doa10-dependent ubiquitination and Ypf1-triggered degradation enable low Zrt1 plasma membrane level, which ensures rate-limiting transport by the low-affinity transporter Zrt2. Upon decline in zinc concentration, cessation of Zrt1 degradation provides rapid increase in plasma membrane level, enabling the cell efficient nutrient uptake.

See also Figure S6 and Table S2.

Genetic studies have identified the core machinery that mediates ERAD of damaged and unassembled proteins (Bagola et al., 2011). Although for some regulated degradation events, such as of Hmg2, execution is mediated by the canonical ERAD factors (Gardner and Hampton, 1999), much less is known of how the abundance of other membrane proteins is controlled. Our analysis combining candidate testing and systematic screening reveals a role of Ypf1 in controlling the level of high-affinity transporters. Moreover, we showed that Doa10 and Dfm1 also have a role in degrading Zrt1, pointing toward a yet-unrecognized branch of the ERAD pathway, which we have termed ERAD-R. Interestingly, human SPP defines a related arm of the ERAD pathway that involves an E3 ubiquitin ligase, TRC8 and Derlin1 (Chen et al., 2014; Stagg et al., 2009). Since at present only few substrates are known for both human SPP and yeast Ypf1, an assessment of the extent of substrate overlap is currently not possible. However, unlike classical ERAD substrates, both known SPP and Ypf1 ERAD substrates have no obvious folding defect (Chen et al., 2014, and this study), potentially leading to usage of a different combination of ER quality control and ERAD factors than for previously described pathways. Since we showed that Ypf1 cleaves Zrt1 into smaller fragments, it is attractive to speculate that by generating unstable membrane species this clipping activity irreversibly triggers removal of polytopic ERAD substrates by the classical dislocation route (see Figure 4E). Previous reports showed that in human tissue culture cells ectopically expressed SPP cleaves within the last TM domain of Presenilin-1 (Moliaka et al., 2004). Likewise, rhomboid proteases have been described to facilitate degradation of polytopic membrane proteins by cleaving either within loops or TM domains (Fleig et al., 2012). Thus, clipping by intramembrane proteases emerges as a universally used mechanism that triggers degradation of selected membrane proteins. Regardless of the precise mechanism, the parallels of how SPP and Ypf1 synergize with the ERAD machinery suggests shared principles that are conserved, and this poses Ypf1 as a valuable model protease to better understand the in vivo functions of SPP in mammalian cells.

Why would yeast or human cells evolve mechanisms to degrade perfectly functional proteins? We show that posttranslational abundance control by Ypf1 provides tight regulation of high-affinity nutrient transporter levels, essential for a robust starvation response (Levy et al., 2011). Whereas transcriptional control and ligand-induced vacuolar degradation are well known to regulate the abundance of these dual transporter systems (Gitan and Eide, 2000; Zhao and Eide, 1996), our study implicates an additional level of regulation on expression levels that is ER centered. First, during growth in nutrient abundance, Ypf1-mediated constitutive degradation of Zrt1 by the ERAD-R pathway ensures that residually translated Zrt1 molecules do not make it to the cell surface, thus enabling early sensing of nutrient depletion (Figure 7D). However, once a starvation response has been induced, alleviation of Ypf1-triggered ERAD enables an immediate accumulation of mature Zrt1 in the ER and subsequently on the plasma membrane, providing a rapid reaction to the nutrient limitation. This is especially important since the transcriptional response of the *ZRT1* promoter only starts within several hours after sensing of a reduction in zinc level and reaches its maximum only after 24 hr (Levy et al., 2011). Hence, although the transcriptional response is very

robust, it is much too slow to enable the cells to create a first line of defense for zinc starvation. Overall, our systemwide analysis suggests that Ypf1 contributes to a general regulatory mechanism in the abundance control of plasma membrane high-affinity transporters.

More generally, focusing on a completely unstudied intramembrane protease of the ER has enabled us to uncover a safelock mechanism utilized by the yeast cell to accurately balance early sensing of nutrient depletion with rapid response to dwindling reservoirs. This proof of concept opens up directions for thinking about substrates of GxGD intramembrane proteases in health and disease. Strikingly, knockdown of the *Caenorhabditis elegans* SPP-type GxGD protease *imp-2* is partially mimicked by cholesterol depletion, and *imp-2* genetically interacts with the lipoprotein receptor *irp-1* (Grigorenko et al., 2004). Thus it is conceivable that loss of accurate nutrient sensing may underlie other events of GxGD aspartyl protease ablation and may have dramatic effects on cellular physiology that were previously not appreciated.

EXPERIMENTAL PROCEDURES

Additional details of the Experimental Procedures can be found in the Supplemental Information.

Yeast Strains

All yeast strains used in this study are based on the W303, BY4741, BY4742, YMS721, or S288c laboratory strains.

Quantitative Proteomics

ER-derived microsomes from WT and *Δypf1* cells were subjected to acetone precipitation, tryptic digestion, and fractionation by strong-cation exchange chromatography. Mass spectrometric measurements were performed with an Orbitrap XL system.

Immunoprecipitation and Inhibitor-Binding Assay

For isolation of Ypf1 complexes, cellular membranes were isolated. Upon solubilization with 2% digitonin, GFP-tagged Ypf1 was immunoprecipitated and analyzed by western blotting. For inhibitor-binding experiments, membranes were lysed with 1% CHAPSO, and Ypf1 was captured using Merck C inhibitor.

Chase Experiments and Western Blotting

Cycloheximide chase and galactose promoter shutoff experiments were performed with cells growing in exponential phase. Total cell extracts prepared by alkaline lysis-trichloracetic acid precipitation and immunoisolated proteins were analyzed by SDS PAGE and western blotting.

Growth, Starvation, and Competition Assays

Growth and starvation assays were recorded using a 96-well plate reader (Tecan). Flow cytometry analysis was performed using BD LSRII flow cytometer, and values were reported as delta from median autofluorescence intensity.

SGA and Systematic Analysis of GFP Library

Synthetic genetic array (SGA) technique was performed with *ypf1* deletion crossed against the GFP library. High-throughput fluorescence microscopy, image analysis, and data processing were performed generating intensity fold change in comparison to WT reference GFP library.

SUPPLEMENTAL INFORMATION

Supplemental Information includes six figures, two tables, and Supplemental Experimental Procedures and can be found with this article at http://dx.doi.org/10.1016/j.molcel.2014.10.012.

AUTHOR CONTRIBUTIONS

D.A. and S.F. designed and performed most experiments and wrote the manuscript. B.S. carried out experiments. A.F. and H.S. carried out the inhibitor-binding assay and helped write the manuscript. M.L.B. and O.S. performed the quantitative proteomics. M.B., I.F., and C.-y.C. helped with experiments. E.K. generated the monoclonal Ypf1 antibody. M.S. and M.K.L. guided the project, designed experiments, and wrote the manuscript.

ACKNOWLEDGMENTS

We thank B. Dobberstein, B. Bukau, M. Seedorf, D. Eide, D. Wolf, J. Brodsky, N. Malchus, H. Lorenz, T. Uhlig, B. Mayer, D. Schlesinger, M. Kafri, M. Carmi, N. Vardi, N. Avraham-Tayar, Y. Pilpel, R. Milo, N. Barkai, G. Basset, and A. Sülzen for reagents, advice, and technical assistance. The work was supported by funds from the Baden-Württemberg Stiftung within the Network of Aging Research (NAR, University of Heidelberg) and the Deutsche Forschungsgemeinschaft (SFB 1036, TP 12) to M.K.L.; Estate of Sunny Howard and Michael Jacobs Charitable Trust fellowships to S.F.; an ERC StG 260395, a Marie Curie Reintegration Grant from the EU (IRG 239224), and the generous support of Ruhman Roberto and Renata to M.S. and S.F.; the Hans and Ilse Breuer Foundation to H.S.; and the Excellence Initiative of the German Federal and State Governments (EXC 294, BIOSS) to O.S.

Received: January 15, 2014
Revised: June 19, 2014
Accepted: October 9, 2014
Published: November 13, 2014

REFERENCES

Adle, D.J., Wei, W., Smith, N., Bies, J.J., and Lee, J. (2009). Cadmium-mediated rescue from ER-associated degradation induces expression of its exporter. Proc. Natl. Acad. Sci. USA *106*, 10189–10194.

Ast, T., Aviram, N., Chuartzman, S.G., and Schuldiner, M. (2014). A cytosolic degradation pathway, prERAD, monitors pre-inserted secretory pathway proteins. J. Cell Sci. *127*, 3017–3023.

Bagola, K., Mehnert, M., Jarosch, E., and Sommer, T. (2011). Protein dislocation from the ER. Biochim. Biophys. Acta *1808*, 925–936.

Baker, D., Hicke, L., Rexach, M., Schleyer, M., and Schekman, R. (1988). Reconstitution of SEC gene product-dependent intercompartmental protein transport. Cell *54*, 335–344.

Beher, D., Fricker, M., Nadin, A., Clarke, E.E., Wrigley, J.D., Li, Y.M., Culvenor, J.G., Masters, C.L., Harrison, T., and Shearman, M.S. (2003). In vitro characterization of the presenilin-dependent gamma-secretase complex using a novel affinity ligand. Biochemistry *42*, 8133–8142.

Breker, M., Gymrek, M., and Schuldiner, M. (2013). A novel single-cell screening platform reveals proteome plasticity during yeast stress responses. J. Cell Biol. *200*, 839–850.

Carvalho, P., Goder, V., and Rapoport, T.A. (2006). Distinct ubiquitin-ligase complexes define convergent pathways for the degradation of ER proteins. Cell *126*, 361–373.

Chen, C.Y., Malchus, N.S., Hehn, B., Stelzer, W., Avci, D., Langosch, D., and Lemberg, M.K. (2014). Signal peptide peptidase functions in ERAD to cleave the unfolded protein response regulator XBP1u. EMBO J. http://dx.doi.org/10.15252/embj.201488208.

De Strooper, B., Saftig, P., Craessaerts, K., Vanderstichele, H., Guhde, G., Annaert, W., Von Figura, K., and Van Leuven, F. (1998). Deficiency of presenilin-1 inhibits the normal cleavage of amyloid precursor protein. Nature *391*, 387–390.

Fleig, L., Bergbold, N., Sahasrabudhe, P., Geiger, B., Kaltak, L., and Lemberg, M.K. (2012). Ubiquitin-dependent intramembrane rhomboid protease promotes ERAD of membrane proteins. Mol. Cell *47*, 558–569.

Gaither, L.A., and Eide, D.J. (2001). Eukaryotic zinc transporters and their regulation. Biometals *14*, 251–270.

Gardner, R.G., and Hampton, R.Y. (1999). A highly conserved signal controls degradation of 3-hydroxy-3-methylglutaryl-coenzyme A (HMG-CoA) reductase in eukaryotes. J. Biol. Chem. *274*, 31671–31678.

Gitan, R.S., and Eide, D.J. (2000). Zinc-regulated ubiquitin conjugation signals endocytosis of the yeast ZRT1 zinc transporter. Biochem. J. *346*, 329–336.

Gitan, R.S., Luo, H., Rodgers, J., Broderius, M., and Eide, D. (1998). Zinc-induced inactivation of the yeast ZRT1 zinc transporter occurs through endocytosis and vacuolar degradation. J. Biol. Chem. *273*, 28617–28624.

Gitan, R.S., Shababi, M., Kramer, M., and Eide, D.J. (2003). A cytosolic domain of the yeast Zrt1 zinc transporter is required for its post-translational inactivation in response to zinc and cadmium. J. Biol. Chem. *278*, 39558–39564.

Grigorenko, A.P., Moliaka, Y.K., Soto, M.C., Mello, C.C., and Rogaev, E.I. (2004). The Caenorhabditis elegans IMPAS gene, imp-2, is essential for development and is functionally distinct from related presenilins. Proc. Natl. Acad. Sci. USA *101*, 14955–14960.

Hampton, R.Y., and Sommer, T. (2012). Finding the will and the way of ERAD substrate retrotranslocation. Curr. Opin. Cell Biol. *24*, 460–466.

Harbut, M.B., Patel, B.A., Yeung, B.K., McNamara, C.W., Bright, A.T., Ballard, J., Supek, F., Golde, T.E., Winzeler, E.A., Diagana, T.T., and Greenbaum, D.C. (2012). Targeting the ERAD pathway via inhibition of signal peptide peptidase for antiparasitic therapeutic design. Proc. Natl. Acad. Sci. USA *109*, 21486–21491.

Huh, W.K., Falvo, J.V., Gerke, L.C., Carroll, A.S., Howson, R.W., Weissman, J.S., and O'Shea, E.K. (2003). Global analysis of protein localization in budding yeast. Nature *425*, 686–691.

Huppa, J.B., and Ploegh, H.L. (1997). The alpha chain of the T cell antigen receptor is degraded in the cytosol. Immunity *7*, 113–122.

Kohlmann, S., Schäfer, A., and Wolf, D.H. (2008). Ubiquitin ligase Hul5 is required for fragment-specific substrate degradation in endoplasmic reticulum-associated degradation. J. Biol. Chem. *283*, 16374–16383.

Lee, S.O., Cho, K., Cho, S., Kim, I., Oh, C., and Ahn, K. (2010). Protein disulphide isomerase is required for signal peptide peptidase-mediated protein degradation. EMBO J. *29*, 363–375.

Lemberg, M.K. (2011). Intramembrane proteolysis in regulated protein trafficking. Traffic *12*, 1109–1118.

Levy, S., Kafri, M., Carmi, M., and Barkai, N. (2011). The competitive advantage of a dual-transporter system. Science *334*, 1408–1412.

Levy-Lahad, E., Wasco, W., Poorkaj, P., Romano, D.M., Oshima, J., Pettingell, W.H., Yu, C.E., Jondro, P.D., Schmidt, S.D., Wang, K., et al. (1995). Candidate gene for the chromosome 1 familial Alzheimer's disease locus. Science *269*, 973–977.

Li, X., Dang, S., Yan, C., Gong, X., Wang, J., and Shi, Y. (2013). Structure of a presenilin family intramembrane aspartate protease. Nature *493*, 56–61.

Loureiro, J., Lilley, B.N., Spooner, E., Noriega, V., Tortorella, D., and Ploegh, H.L. (2006). Signal peptide peptidase is required for dislocation from the endoplasmic reticulum. Nature *441*, 894–897.

Manolaridis, I., Kulkarni, K., Dodd, R.B., Ogasawara, S., Zhang, Z., Bineva, G., O'Reilly, N., Hanrahan, S.J., Thompson, A.J., Cronin, N., et al. (2013). Mechanism of farnesylated CAAX protein processing by the intramembrane protease Rce1. Nature *504*, 301–305.

Miyashita, H., Maruyama, Y., Isshiki, H., Osawa, S., Ogura, T., Mio, K., Sato, C., Tomita, T., and Iwatsubo, T. (2011). Three-dimensional structure of the signal peptide peptidase. J. Biol. Chem. *286*, 26188–26197.

Moliaka, Y.K., Grigorenko, A., Madera, D., and Rogaev, E.I. (2004). Impas 1 possesses endoproteolytic activity against multipass membrane protein substrate cleaving the presenilin 1 holoprotein. FEBS Lett. *557*, 185–192.

Narayanan, S., Sato, T., and Wolfe, M.S. (2007). A C-terminal region of signal peptide peptidase defines a functional domain for intramembrane aspartic protease catalysis. J. Biol. Chem. *282*, 20172–20179.

Nyborg, A.C., Kornilova, A.Y., Jansen, K., Ladd, T.B., Wolfe, M.S., and Golde, T.E. (2004). Signal peptide peptidase forms a homodimer that is labeled by an active site-directed gamma-secretase inhibitor. J. Biol. Chem. *279*, 15153–15160.

Ponting, C.P., Hutton, M., Nyborg, A., Baker, M., Jansen, K., and Golde, T.E. (2002). Identification of a novel family of presenilin homologues. Hum. Mol. Genet. *11*, 1037–1044.

Radisky, D., and Kaplan, J. (1999). Regulation of transition metal transport across the yeast plasma membrane. J. Biol. Chem. *274*, 4481–4484.

Schrul, B., Kapp, K., Sinning, I., and Dobberstein, B. (2010). Signal peptide peptidase (SPP) assembles with substrates and misfolded membrane proteins into distinct oligomeric complexes. Biochem. J. *427*, 523–534.

Sherrington, R., Rogaev, E.I., Liang, Y., Rogaeva, E.A., Levesque, G., Ikeda, M., Chi, H., Lin, C., Li, G., Holman, K., et al. (1995). Cloning of a gene bearing missense mutations in early-onset familial Alzheimer's disease. Nature *375*, 754–760.

Stagg, H.R., Thomas, M., van den Boomen, D., Wiertz, E.J., Drabkin, H.A., Gemmill, R.M., and Lehner, P.J. (2009). The TRC8 E3 ligase ubiquitinates MHC class I molecules before dislocation from the ER. J. Cell Biol. *186*, 685–692.

Steiner, H., Kostka, M., Romig, H., Basset, G., Pesold, B., Hardy, J., Capell, A., Meyn, L., Grim, M.L., Baumeister, R., et al. (2000). Glycine 384 is required for presenilin-1 function and is conserved in bacterial polytopic aspartyl proteases. Nat. Cell Biol. *2*, 848–851.

Stolz, A., Schweizer, R.S., Schäfer, A., and Wolf, D.H. (2010). Dfm1 forms distinct complexes with Cdc48 and the ER ubiquitin ligases and is required for ERAD. Traffic *11*, 1363–1369.

Torres-Arancivia, C., Ross, C.M., Chavez, J., Assur, Z., Dolios, G., Mancia, F., and Ubarretxena-Belandia, I. (2010). Identification of an archaeal presenilin-like intramembrane protease. PLoS ONE *5*, http://dx.doi.org/10.1371/journal.pone.0013072.

Tyler, R.E., Pearce, M.M., Shaler, T.A., Olzmann, J.A., Greenblatt, E.J., and Kopito, R.R. (2012). Unassembled CD147 is an endogenous endoplasmic reticulum-associated degradation substrate. Mol. Biol. Cell *23*, 4668–4678.

Weihofen, A., Binns, K., Lemberg, M.K., Ashman, K., and Martoglio, B. (2002). Identification of signal peptide peptidase, a presenilin-type aspartic protease. Science *296*, 2215–2218.

Wolfe, M.S., De Los Angeles, J., Miller, D.D., Xia, W., and Selkoe, D.J. (1999). Are presenilins intramembrane-cleaving proteases? Implications for the molecular mechanism of Alzheimer's disease. Biochemistry *38*, 11223–11230.

Zhang, Y., Nijbroek, G., Sullivan, M.L., McCracken, A.A., Watkins, S.C., Michaelis, S., and Brodsky, J.L. (2001). Hsp70 molecular chaperone facilitates endoplasmic reticulum-associated protein degradation of cystic fibrosis transmembrane conductance regulator in yeast. Mol. Biol. Cell *12*, 1303–1314.

Zhao, H., and Eide, D. (1996). The yeast ZRT1 gene encodes the zinc transporter protein of a high-affinity uptake system induced by zinc limitation. Proc. Natl. Acad. Sci. USA *93*, 2454–2458.